

Phase diagram of diblock copolymer melt in dimension $d=5$

M. Dziecielski,¹ K. Lewandowski,¹ and M. Banaszak^{1,*}

¹*Faculty of Physics, A. Mickiewicz University
ul. Umultowska 85, 61-614 Poznan, Poland*

(Dated: January 26, 2022)

Abstract

Using self-consistent field theory (SCFT) in spherical unit cells of various dimensionalities, D , a phase diagram of a diblock, A - b - B , is calculated in 5 dimensional space, $d=5$. This is an extension of a previous work for $d=4$. The phase diagram is parameterized by the chain composition, f , and incompatibility between A and B , quantified by the product χN . We predict 5 stable nanophases: layers, cylinders, 3D spherical cells, 4D spherical cells, and 5D spherical cells. In the strong segregation limit, that is for large χN , the order-order transition compositions are determined by the strong segregation theory (SST) in its simplest form. While the predictions of the SST theory are close to the corresponding SCFT extrapolations for $d = 4$, the extrapolations for $d = 5$ significantly differ from them. We find that the S_5 nanophase is stable in a narrow strip between ordered S_4 nanophase and the disordered phase. The calculated order-disorder transition lines depend weakly on d , as expected.

* mbanasz@amu.edu.pl Corresponding Author

I. INTRODUCTION

Diblock copolymer (DBC), A - b - B , melts consist of 2 types of segments, A and B , arranged in 2 corresponding blocks. Those melts can self-assemble in $3d$ into various spatially-ordered nanophases, such as layers, (L), hexagonally packed cylinders, (C), gyroid nanostructures, (G), with the $Ia\bar{3}d$ symmetry, and cubically packed (either body-centered or closely packed) spherical cells (S), depending on the chain composition, f (f is the fraction of A -segments; $1 - f$ is the fraction of B -segments), degree of polymerization (number of segments), N , and the temperature-related χ parameter [1, 2]. Recently, an additional O^{70} -phase has been reported [3, 4], but it is stable in a very small region of the phase diagram. Those nanophases can be transformed into a disordered phase, for example, upon heating. It is of great interest to determine a phase diagram of such melts exhibiting order-disorder transition (ODT) lines, also referred to as binodals of microphase separation transition (MST), and order-order transition (OOT) lines. This task has been largely achieved for 3-dimensional (bulk) diblock melts by accumulating results from numerous experimental and theoretical studies [5–12], also for $2d$ diblock copolymer melts [13].

The L , C , and S nanophases are known as classical, whereas G and O^{70} nanonophases are referred to as non-classical, or sometimes complex. The Wigner-Seitz cell of a classical phase can be approximated by D -dimensional sphere, S_D , both in the real \vec{r} -space and the reciprocal \vec{k} -space. Within this approximation, known as Unit Cell Approximation (UCA), the L , C , S nanophases correspond to S_1 , S_2 , and S_3 , respectively, and the spacial distribution of chain segments can be mapped with a single radial variable, r , as shown in Table I. The classical phases can be easily generalized to higher dimensions, in particular for $d = 5$ we can have 5 nanophases S_D , with dimensionality, D , ranging from 1 to 5.

It is interesting that a mean-field (MF) theory applied to copolymer melts [8, 14, 15], known as the Self-Consistent Field Theory (SCFT), is successful in predicting diblock phase diagrams resembling the experimental ones, as shown, for example, in ref [16]. The SCFT approach is based on the assumption that coarse-grained polymer chains in dense melts are Gaussian (Flory's theorem [17]), and on the MF approximation which selects the dominant contribution in the appropriate partition function, thus neglecting fluctuations.

Because, in the MF theories, it is sufficient to know the composition, f , and the product χN in order to foresee the nanophase [5, 15, 18], the diblock phase diagram can be mapped in

TABLE I. Unit cell equations of D -dimensionality; equations are supplemented with the unconstrained variables for corresponding d 's (2, 3, 4 and 5); * indicates the absence of unconstrained variables; imp indicates that the nanophase for this d is impossible

D	nanophase	cell equation	d=2	d=3	d=4	d=5	radial coordinate
1	L (S_1)	$x^2 < R^2$	y	y, z	y, z, t	y, z, t, v	$r = x $
2	C (S_2)	$x^2 + y^2 < R^2$	*	z	z, t	z, t, v	$r = \sqrt{x^2 + y^2}$
3	S_3	$x^2 + y^2 + z^2 < R^2$	imp	*	t	t, v	$r = \sqrt{x^2 + y^2 + z^2}$
4	S_4	$x^2 + y^2 + z^2 + t^2 < R^2$	imp	imp	*	v	$r = \sqrt{x^2 + y^2 + z^2 + t^2}$
5	S_5	$x^2 + y^2 + z^2 + t^2 + v^2 < R^2$	imp	imp	imp	*	$r = \sqrt{x^2 + y^2 + z^2 + t^2 + v^2}$

$(f, \chi N)$ -plane. The MF theories exist in many variations, both in real space (\vec{r} -space)[6, 7, 9] and Fourier space (\vec{k} -space) [2, 8].

In addition, we intend to compare the phase boundaries calculated by the SCFT (and extrapolated to the strong segregation limit) with the strong segregation theory (SST) for diblock melts, developed by Semenov [19], in which the free energy of the nanophase has three contributions, the interfacial tension and the stretching (of entropic origin) energies of the A and B blocks. These energies can be approximated by simple expressions, allowing the calculation of the OOT compositions in the SST. The main goal of this paper is to construct a phase diagram of a copolymer melt for $d = 5$, applying the SCFT method with the UCA in r -space, as presented in [6–8]. Specifically, we intend to determine the area in $(f, \chi N)$ -space, in which the S_5 phase is stable, by varying both the radius, R , of the unit cell and the dimensionality, D .

In previous work[20] we calculated the phase diagram of the diblock copolymer melt for $d = 4$, and managed to answer the following questions:

1. is the S_4 nanophase stable?
2. what is the sequence of nanophases, upon changing f ?
3. are the binodals (ODT lines) shifted as we vary d from 1 to 4?
4. what are the strong segregation limits of the OOT lines for $d = 4$?

The answers were as follows:

1. the nanophase S_4 is stable within a relatively narrow strip between the S_3 nanophase and the disordered phase,
2. the sequence of nanophases appropriate for the UCA in $3d$ is preserved, starting from $f = 1/2$, L , C , S_3 , and there is an additional S_4 nanophase in $4d$,
3. the ODT binodals depend weakly on d , and they are shifted as d is varied,
4. the SST compositions, $f_{L/C}$, f_{C/S_3} , and f_{S_3/S_4} are close to the corresponding extrapolations from the self-consistent field theory.

In this work, similarly as in ref 20, the following questions are posed:

1. is the S_5 nanophase stable?
2. what is the position of the S_5 nanophase in sequence of phases, upon changing f ?
3. are the binodals (ODT lines) shifted as we vary d from 4 to 5?
4. what are the strong segregation limits of the OOT lines for $d=5$?

II. METHOD

The incompressible copolymer melt is modeled as a collection of n diblock chains confined in volume V . Each chain, labeled $\alpha = 1, 2, \dots, n$, can take any Gaussian configuration (in accordance with the Flory's Theorem [17]) parameterized from $s=0$ to $s=f$ for A -segments, and from $s=f$ to $s=1$ for B -segments. Up to a multiplicative constant, the partition function for a *single* Gaussian chain in external fields $W_A(\mathbf{r})$ and $W_B(\mathbf{r})$ acting on segments A and B, respectively, is

$$\mathcal{Q}[W_A, W_B] \equiv \int \tilde{\mathcal{D}}\mathbf{r}_\alpha(\cdot) \exp \left[- \int_0^f ds W_A(\mathbf{r}_\alpha(s)) - \int_f^1 ds W_B(\mathbf{r}_\alpha(s)) \right] \quad (1)$$

The path integral, $\int \tilde{\mathcal{D}}\mathbf{r}_\alpha(\cdot)$, is taken over single-chain trajectories, $\mathbf{r}_\alpha(s)$, with Wiener measure expressed as $\tilde{\mathcal{D}}\mathbf{r}_\alpha = \mathcal{D}\mathbf{r}_\alpha P[\mathbf{r}_\alpha; 0, 1]$, and

$$P[\mathbf{r}_\alpha; s_1, s_2] \propto \exp \left[- \frac{3}{2Na^2} \int_{s_1}^{s_2} ds \left| \frac{d}{ds} \mathbf{r}_\alpha(s) \right|^2 \right] \quad (2)$$

Note that a is the segment size, and Na^2 is the mean squared end-to-end distance of a Gaussian chain. By Kac-Feynman theorem, eq 1 can be related to a Fokker-Planck partial differential equation[2], known also as modified diffusion equation (MDE) and shown with appropriate details below (eqs 15 and 16).

Segments A and B interact via the χ parameter which provides an effective measure of incompatibility between them[17]. Evaluation of the full partition function of n interacting diblock chains, shown below (eq 3), is a highly challenging task, involving many-body interactions, both intermolecular and intramolecular.

$$Z = \int \prod_{\alpha=1}^n \tilde{\mathcal{D}}\mathbf{r}_\alpha \delta[1 - \hat{\phi}_A - \hat{\phi}_B] \exp \left[- \chi \rho_0 \hat{\phi}_A \hat{\phi}_B \right] \quad (3)$$

where δ -function enforces incompressibility (the melt is assumed to be incompressible), and

$$\hat{\phi}_A(\mathbf{r}) = \frac{N}{\rho_0} \sum_{\alpha=1}^n \int_0^f ds \delta(\mathbf{r} - \mathbf{r}_\alpha(s)) \quad (4)$$

$$\hat{\phi}_B(\mathbf{r}) = \frac{N}{\rho_0} \sum_{\alpha=1}^n \int_f^1 ds \delta(\mathbf{r} - \mathbf{r}_\alpha(s)) \quad (5)$$

are the microscopic segments densities of A and B , respectively; $\rho_0 = nN/V$ is the segment number density. After replacing microscopic segment (or particle) densities with a variety

of fields [2, 6–8], by inserting and spectrally decomposing the appropriate δ -functionals, the partition function of an incompressible diblock melt is

$$Z = \mathcal{N} \int \mathcal{D}\phi_A(\cdot) \mathcal{D}W_A(\cdot) \mathcal{D}\phi_B(\cdot) \mathcal{D}W_B(\cdot) \mathcal{D}\Psi(\cdot) \exp \left[-\frac{F[\phi_A, W_A, \phi_B, W_B, \Psi]}{k_B T} \right] \quad (6)$$

where \mathcal{N} is a normalization factor. The functional integral is taken over the relevant fields $\phi_A(\mathbf{r})$, $W_A(\mathbf{r})$, $\phi_B(\mathbf{r})$, $W_B(\mathbf{r})$, and $\Psi(\mathbf{r})$, with the free energy functional, $F[\phi_A, W_A, \phi_B, W_B, \Psi]$, including the single chain partition function (in external fields $W_A(\mathbf{r})$ and $W_B(\mathbf{r})$), as shown below

$$\begin{aligned} \frac{F[\phi_A, W_A, \phi_B, W_B, \Psi]}{nk_B T} &\equiv -\ln \frac{\mathcal{Q}}{V} + V^{-1} \int d\mathbf{r} [N\chi\phi_A(\mathbf{r})\phi_B(\mathbf{r}) \\ &\quad - W_A(\mathbf{r})\phi_A(\mathbf{r}) - W_B(\mathbf{r})\phi_B(\mathbf{r}) \\ &\quad - \Psi(\mathbf{r})(1 - \phi_A(\mathbf{r}) - \phi_B(\mathbf{r}))] \end{aligned} \quad (7)$$

Fields $\phi_A(\mathbf{r})$ and $\phi_B(\mathbf{r})$ are associated with normalized concentration profiles of A and B , and fields $W_A(\mathbf{r})$ and $W_B(\mathbf{r})$ with chemical potential fields acting on A and B , respectively; field $\Psi(\mathbf{r})$ enforces incompressibility. Evaluating functional integrals in eq 6 is a challenging task which, in principle, can be performed by field theoretic simulations as proposed and implemented by Fredrickson and coworkers[2, 11]. A simpler, but approximate, approach is based on the mean-field idea, where the dominant, and in fact only, contribution to the functional integral in eq 6 comes from the fields satisfying the saddle point condition expressed as the following set of equations:

$$\frac{\delta F}{\delta\phi_A} = \frac{\delta F}{\delta\phi_B} = \frac{\delta F}{\delta W_A} = \frac{\delta F}{\delta W_B} = \frac{\delta F}{\delta\Psi} = 0 \quad (8)$$

Performing the above functional derivatives yields

$$W_A(\mathbf{r}) = N\chi\phi_B(\mathbf{r}) + \Psi(\mathbf{r}) \quad (9)$$

$$W_B(\mathbf{r}) = N\chi\phi_A(\mathbf{r}) + \Psi(\mathbf{r}) \quad (10)$$

$$1 = \phi_A(\mathbf{r}) + \phi_B(\mathbf{r}) \quad (11)$$

$$\phi_A(\mathbf{r}) = \frac{V}{\mathcal{Q}} \int_0^f ds q(\mathbf{r}, s) q^\dagger(\mathbf{r}, s) \quad (12)$$

$$\phi_B(\mathbf{r}) = \frac{V}{\mathcal{Q}} \int_f^1 ds q(\mathbf{r}, s) q^\dagger(\mathbf{r}, s) \quad (13)$$

where \mathcal{Q}/V can be calculated as

$$\frac{\mathcal{Q}}{V} = \frac{1}{V} \int d\mathbf{r} q(\mathbf{r}, 1) \quad (14)$$

and $q(\mathbf{r}, s)$ is the forward chain propagator which is the solution of the following modified diffusion equation

$$\begin{aligned}\frac{\partial q}{\partial s} &= \frac{1}{6}Na^2\nabla^2 q - W_A(\mathbf{r})q, \quad 0 \leq s \leq f \\ \frac{\partial q}{\partial s} &= \frac{1}{6}Na^2\nabla^2 q - W_B(\mathbf{r})q, \quad f \leq s \leq 1\end{aligned}\tag{15}$$

with the initial condition $q(\mathbf{r}, 0) = 1$. Similarly $q^\dagger(\mathbf{r}, s)$ is the backward chain propagator which is the solution of the conjugate modified diffusion equation:

$$\begin{aligned}-\frac{\partial q^\dagger}{\partial s} &= \frac{1}{6}Na^2\nabla^2 q^\dagger - W_A(\mathbf{r})q^\dagger, \quad 0 \leq s \leq f \\ -\frac{\partial q^\dagger}{\partial s} &= \frac{1}{6}Na^2\nabla^2 q^\dagger - W_B(\mathbf{r})q^\dagger, \quad f \leq s \leq 1\end{aligned}\tag{16}$$

with the initial condition $q^\dagger(\mathbf{r}, 1) = 1$.

While the set of equations 9, 10, 11, 12, and 13 can be solved, in principle, in a self-consistent manner, it is difficult to solve this set without some additional assumptions. First, we assume that the melt forms a spatially ordered nanophase. Second, we use the UCA which is a considerable simplification, limiting our attention to a single D-dimensional spherical cell of radius R , and volume V . All fields, within this cell, have radial symmetry, which reduces this problem computationally to a single radial coordinate, r . The unconstrained spatial variables, specified in Table I for each d , become computationally irrelevant. Thus eq 14 can be rewritten as

$$\frac{\mathcal{Q}}{V} = D \frac{\int_0^R r^{D-1} q(r, 1) dr}{R^D}\tag{17}$$

Note that the factor, D , in front of the above integral originates from the ratio of the area of a sphere with radius 1 to the volume of a spherical cell with the same radius, both in D dimensions.

While in integrals (eqs 12, 13 and 14) we replace \mathbf{r} with r , and $d\mathbf{r}/V$ with $Dr^{D-1}dr/R^D$, in the modified diffusion equations, 15 and 16, we replace \mathbf{r} with r and use the spherically symmetric form of the Laplacian

$$\nabla^2 f = \frac{\partial^2 f}{\partial r^2} + \frac{D-1}{r} \frac{\partial f}{\partial r}\tag{18}$$

and similarly, in equations for both propagators $q(r, s)$ and $q^\dagger(r, s)$, we replace \mathbf{r} with r . Obviously the solution depends on radius, R , and dimensionality, $D = 1, 2, 3, 4$ and 5, corresponding to 5 different nanophases, shown in Table I. We use the Crank-Nicholson

scheme[20] to solve iteratively the modified diffusion equations (eqs 15 and 16) in their radial form, until the self-consistency condition is met, obtaining the saddle point fields, $\overline{\phi}_A(r)$, $\overline{\phi}_B(r)$, $\overline{W}_A(r)$ and $\overline{W}_B(r)$ for a given R and D . In the MF approximation, the free energy functional becomes the free energy, and therefore we calculate the reduced free energy (per chain in $k_B T$ units) by substituting the saddle point fields into eq 7:

$$\frac{F(R, D)}{nk_B T} \equiv -\ln \frac{Q}{V} + \frac{D}{R^D} \int_0^R r^{D-1} [N\chi \overline{\phi}_A(r) \overline{\phi}_B(r) - \overline{W}_A(r) \overline{\phi}_A(r) - \overline{W}_B(r) \overline{\phi}_B(r)] dr \quad (19)$$

III. RESULTS AND DISCUSSION

Since in the MF theory, the stability of a nanophase depends on the product χN and composition, f , we start, at a given point of the phase diagram, $(f, \chi N)$, with numerical calculation of $F(R, D)$ (eq 19) for various D 's (1, 2, 3, 4, and 5) and R 's. In order to solve the MDE's (eqs 15 and 16) we use up to $N_T = 160$ and up to $N_R = 800$ steps for the "time", s , and space, r , variables, respectively.

Numerically, we find R and D which minimize $F(R, D)$, and this allows us to determine the dimensionality, D , of the most stable nanophase, and therefore the most favorable nanophase itself, using the correspondence from Table I. But the free energy of this nanophase has to be compared to that of the disordered phase. Therefore, we calculate the difference

$$\frac{\Delta F}{nk_B T} \equiv \frac{F}{nk_B T} - \frac{F_{dis}}{nk_B T} \quad (20)$$

where F_{dis} is the free energy of the disordered phase:

$$\frac{F_{dis}}{nk_B T} = N\chi f(1 - f) \quad (21)$$

If ΔF is negative then the appropriate nanophase is thermodynamically stable for the point considered, $(f, \chi N)$; otherwise the system is the disordered phase. For example, in Figure 1 we compare $\Delta F/(nk_B T)$ for $d = 4$ and $d = 5$ as a function of f , at $\chi N = 50$. The intersection of those free energy curves occurs at $f_{S_4/S_5} = 0.10418$, as also indicated in Table II.

This procedure allows us to map the DBC melt phase diagram for $d = 5$ in the $(f, \chi N)$ -plane, as shown in Fig 2. Since there is a mirror symmetry with respect to $f = 0.5$ ($f \rightarrow 1 - f$, A can be exchanged with B), we show the resultant nanophases only from $f = 0$ to 0.5, and the following phase sequence is observed: L , C , S_3 , S_4 , S_5 and the disordered phase; the corresponding data for those lines is presented in Table II. A new nanophase, S_5 , is observed in a relatively narrow strip between the S_4 phase and disordered phase. This is the main result of this paper. We extrapolate the calculated OOT lines, $f_{L/C}$, f_{C/S_3} , f_{S_3/S_4} , f_{S_4/S_5} to the strong segregation limit, that is we estimate them as $\chi N \rightarrow \infty$ (or $1/(\chi N) \rightarrow 0$), fitting to the following function:

$$f(\chi N) = f^0 + \frac{g^0}{\chi N} \quad (22)$$

as used in referenced [9] and [20], where f^0 is the extrapolation to the strong segregation limit, and g^0 is a fitting parameter. The resultant limits, $f_{L/C}^0$, f_{C/S_3}^0 , f_{S_3/S_4}^0 , as determined in ref 20 and f_{S_4/S_5}^0 (determined in this paper) are compared to the SST f 's, as shown in Table III. The discrepancy between the SST and the present SCFT with the UCA, for $f_{L/C}$ and f_{C/S_3} is within 2% error, as also reported in [9], and the discrepancy for f_{S_3/S_4} is about 10%. However, the difference between the extrapolated $f_{S_4/S_5}^0 = 0.01$ and the calculated $f_{S_4/S_5} = 0.00018$ (from SST) is much larger. Since the SCFT is more advanced and accurate theory than the SST (the SCFT is a full mean field theory, and the SST is an approximation of the mean field theory which is meaningful only at strong segregations), we demonstrate that the area of stability for the S_5 phase is mostly likely to be significantly larger than that predicted from the SST.

While spinodals for the ODT calculated with random-phase approximation (RPA) [5] are the same for $d = 2, 3, 4$, and 5 the binodals (the ODT lines), calculated in this work, depend on d as shown in Fig 3. The binodals depend weakly on d , and they are particularly close to each other in the vicinity of $f_A = 1/2$ (symmetric diblock), and therefore we show them in a narrow window (from 70 to 75 in χN , that is away from $f = 1/2$) in the inset of Fig 3. We observe the sequence of binodals, as shown in inset of Fig 3. For $f = 1/2$ the RPA spinodal is at $(\chi N)_c \approx 10.4949$, and the calculated binodals (for $d=2, 3, 4$ and 5) also converge to this point within the numerical accuracy. Similarly, the OOT lines seem to converge to $(\chi N)_c$ for $f = 0.5$.

IV. CONCLUSIONS

Using a self-consistent field theory in spherical unit cells of various dimensionalities, $D=1, 2, 3, 4$ and 5, we calculate phase diagram of a diblock, A - b - B , copolymer melt in 5-dimensional space, $d=5$. The phase diagram is parameterized by the chain composition, f , and incompatibility between A and B , quantified by the product χN . We predict 5 stable nanophases: layers, cylinders, 3D spherical cells, 4D spherical cells and 5D spherical cells, and calculate both order-disorder and order-order transition lines. In the strong segregation limit, that is for large χN , the OOT compositions, $f_{L/C}$, f_{C/S_3} , f_{S_3/S_4} and f_{S_4/S_5} are determined by the strong segregation theory. While $f_{L/C}$, f_{C/S_3} , and f_{S_3/S_4} are close to the corresponding extrapolations from the self-consistent field theory, as shown known in the

χN	$f_{L/C}$	f_{C/S_3}	f_{S_3/S_4}	f_{S_4/S_5}	f_{ODT}
20	0.36797	0.25210	0.22436	0.21461	0.20541
30	0.34531	0.20048	0.16643	0.15475	0.14434
40	0.33601	0.17474	0.13631	0.12379	0.11347
50	0.33120	0.15988	0.11714	0.10418	0.09439
60	0.32828	0.15059	0.10379	0.09086	0.08086
70	0.32629	0.14452	0.09387	0.08043	0.07143
80	0.32482	0.14057	0.08698	0.07143	0.06383
90	0.32392	0.13737	0.08029	0.06556	0.05789
100	0.32303	0.13510	0.07535	0.05983	0.05332

TABLE II. The ODT and OOT lines for selected χN 's

TABLE III. The OOT lines from the full SCFT[9] and UCA extrapolated to infinite χN 's compared to the SST results

Method	$f_{L/C}^0$	f_{C/S_3}^0	f_{S_3/S_4}^0 [20]	f_{S_4/S_5}^0
full SCFT [9]	0.3100	0.1050	-	-
UCA	0.3150	0.1149	0.0306	0.010
SST	0.2999	0.1172	0.0336	0.00018

previous study [20], the f_{S_4/S_5} extrapolation does not agree with the SST predictions. We find that the S_5 nanophase is stable in a narrow strip between ordered S_4 nanophase and the disordered phase. The calculated binodals (ODT lines) depend weakly on d , as expected.

ACKNOWLEDGMENTS

We acknowledge a computational grant from the Poznan Supercomputing and Networking Center (PCSS).

-
- [1] I. W. Hamley, *Developments in Block Copolymer Science and Technology* (John Wiley & Sons, Berlin, 2004).
 - [2] G. H. Fredrickson, *The Equilibrium Theory of Inhomogeneous Polymers* (Clarendon Press, Oxford, 2006).
 - [3] T. S. Bailey, C. M. Hardy, T. H. Epps, and F. S. Bates, *Macromolecules* **35**, 7007 (2002).
 - [4] M. Takenaka, T. Wakada, S. Akasaka, S. Nishisuji, K. Saijo, H. Shimizu, M. I. Kim, and H. Hasegawa, *Macromolecules* **40**, 4399 (2007).
 - [5] L. Leibler, *Macromolecules* **13**, 1602 (1980).
 - [6] M. Banaszak and M. D. Whitmore, *Macromolecules* **25**, 3406 (1992).
 - [7] J. D. Vavasour and M. D. Whitmore, *Macromolecules* **25**, 5477 (1992).
 - [8] M. W. Matsen and M. Schick, *Phys. Rev. Lett.* **72**, 2660 (1994).
 - [9] M. W. Matsen and M. D. Whitmore, *J. Chem. Phys.* **105**, 9698 (1996).
 - [10] M. W. Matsen, *J. Chem. Phys.* **114**, 10528 (2001).
 - [11] E. M. Lennon, K. Katsov, and G. H. Fredrickson, *Phys. Rev. Lett.* **101**, 138302 (2008).
 - [12] T. Taniguchi, *Journal of the Physical Society of Japan* **78**, 041009 (2009).
 - [13] I. W. Hamley, *Progress in Polymer Science* **34**, 1161 (2009).
 - [14] M. W. Matsen, in *Soft Condensed Matter*, Vol. 1, edited by G. Gompper and M. Schick (John Wiley & Sons, Berlin, 2005).
 - [15] E. W. Cochran, C. J. Garcia-Cervera, and G. H. Fredrickson, *Macromolecules* **39**, 2449 (2006).
 - [16] A. K. Khandpur, S. Forster, F. S. Bates, I. W. Hamley, A. J. Ryan, W. Bras, K. Almdal, and K. Mortensen, *Macromolecules* **28**, 8796 (1995).
 - [17] P. G. de Gennes, *Scaling Concepts in Polymer Physics* (Cornell University Press, Ithaca, 1979).
 - [18] M. W. Matsen, *J. Phys.: Condens. Matter* **14**, R21 (2002).
 - [19] A. N. Semenov, *Sov. Phys. JETP* **61**, 733 (1985).
 - [20] M. Banaszak, A. Koper, K. Lewandowski, and P. Knychala, Submitted.

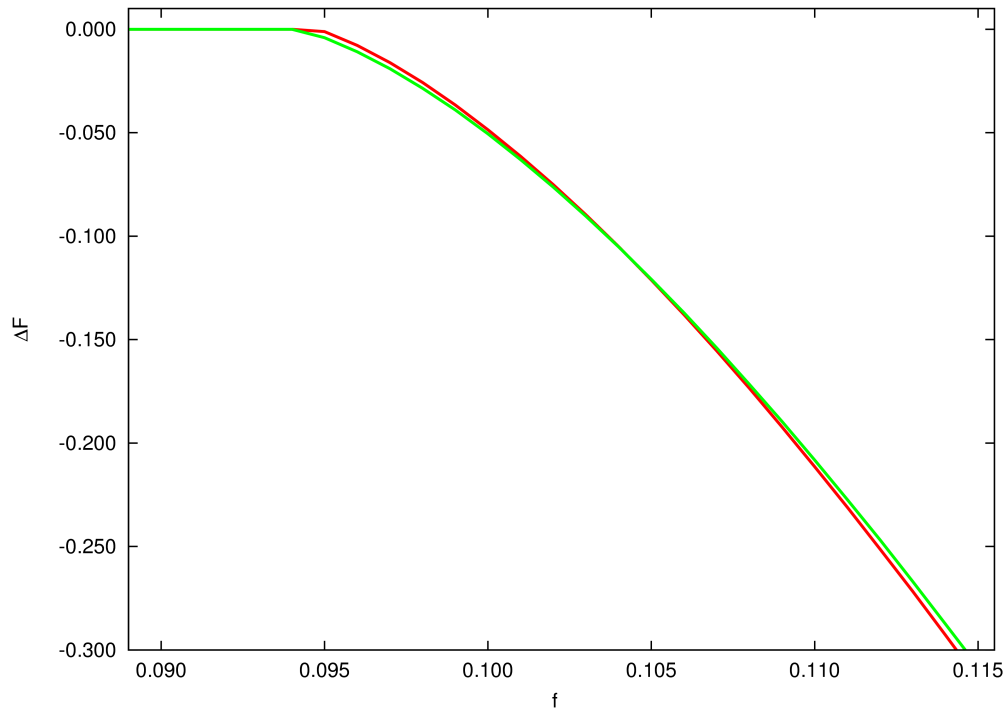


FIG. 1. ΔF (in $nk_B T$ units) as a function of f for $\chi N = 50$. Red line indicates the results for the S_4 nanostructure and green line for the S_5 nanostructure. The lines intersect at $f_{S_4/S_5} = 0.10418$.

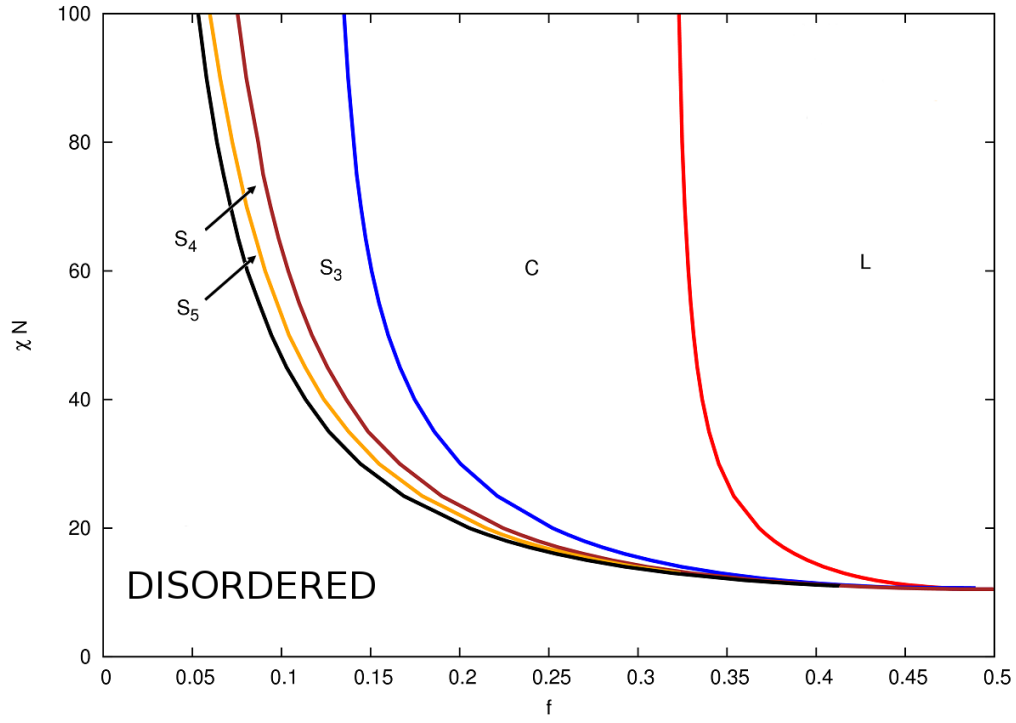


FIG. 2. DBC phase diagram in 5d: L , C , S_3 , S_4 , and S_5 indicate corresponding nanophases; the disordered phase is also shown.

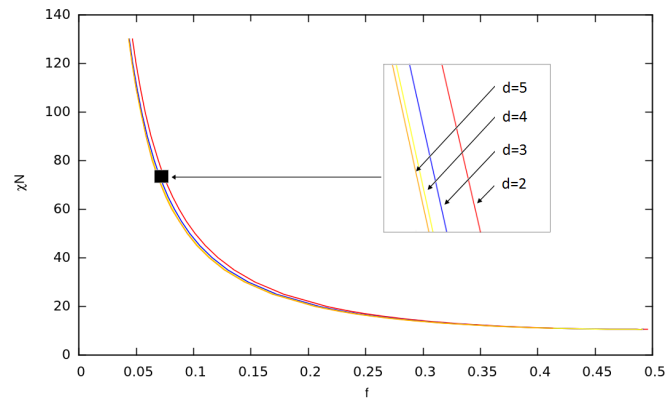


FIG. 3. The ODT lines for $d=2, 3, 4$ and 5 . The inset is from $\chi N = 70$ to 75 .